General Disclaimer

One or more of the Following Statements may affect this Document

- This document has been reproduced from the best copy furnished by the organizational source. It is being released in the interest of making available as much information as possible.

- This document may contain data, which exceeds the sheet parameters. It was furnished in this condition by the organizational source and is the best copy available.

- This document may contain tone-on-tone or color graphs, charts and/or pictures, which have been reproduced in black and white.

- This document is paginated as submitted by the original source.

- Portions of this document are not fully legible due to the historical nature of some of the material. However, it is the best reproduction available from the original submission.

Produced by the NASA Center for Aerospace Information (CASI)

JPL PUBLICATION 84-91

Large Amplitude Forcing of a High Speed Two-Dimensional Jet

L. Bernal
V. Sarohia

December 15, 1984

Large Amplitude Forcing of a High Speed Two-Dimensional Jet

L. Bernal
V. Sarohia

December 15, 1984

1. Report No. 84-91	2. Government Accession No.	3. Recipient's Catalog No.

4. Title and Subtitle	5. Report Date
Large Amplitude Forcing of a High Speed Two-Dimensional Jet	December 15, 1984
	6. Performing Organization Code

7. Author(s) L. Bernal and V. Sarohia	8. Performing Organization Report No.

9. Performing Organization Name and Address	10. Work Unit No.
JET PROPULSION LABORATORY California Institute of Technology 4800 Oak Grove Drive Pasadena, California 91109	11. Contract or Grant No. NAS7-918
	13. Type of Report and Period Covered January 1982 - December 1983

12. Sponsoring Agency Name and Address	
NATIONAL AERONAUTICS AND SPACE ADMINISTRATION Washington, D.C. 20546	14. Sponsoring Agency Code RE65 CY-505-43-00-03-69

15. Supplementary Notes

This report was prepared by the Jet Propulsion Laboratory for the U.S. Department of the Navy and for the National Aeronautics and Space Administration.

16. Abstract

The effect of large amplitude forcing on the growth of a high speed two-dimensional jet has been investigated experimentally. Two forcing techniques were utilized: mass flow oscillations and a mechanical system. The mass flow oscillation tests were conducted at Strouhal numbers from 0.00052 to 0.045, and peak-to-peak amplitudes up to 50 percent of the mean exit velocity. The exit Mach number was varied in the range 0.15 to 0.8. The corresponding Reynolds numbers were 8,400 and 45,000. The results indicate no significant change of the jet growth rate or centerline velocity decay compared to the undisturbed free-jet. The mechanical forcing system consists of two counter-rotating hexagonal cylinders located parallel to the span of the nozzle. Forcing frequencies up to 1,500 Hz were tested. Both symmetric and antisymmetric forcing can be implemented. The results for antisymmetric forcing showed a significant (75 percent) increase of the jet growth rate at an exit Mach number of 0.25 and a Strouhal number of 0.019. At higher rotational speeds, the jet deflected laterally. A deflection angle of 39° with respect to the centerline was measured at the maximum rotational speed.

17. Key Words (Selected by Author(s))	18. Distribution Statement
Aerodynamics; Aircraft Propulsion and Power; Air-Breathing Engines	Unclassified; unlimited

19. Security Classif. (of this report)	20. Security Classif. (of this page)	21. No. of Pages	22. Price
Unclassified	Unclassified		

ABSTRACT

The effect of large amplitude forcing on the growth of a high speed two-dimensional jet has been investigated experimentally. Two forcing techniques were utilized: mass flow oscillations and a mechanical system. The mass flow oscillation tests were conducted at Strouhal numbers from 0.00052 to 0.045, and peak-to-peak amplitudes up to 50 percent of the mean exit velocity. The exit Mach number was varied in the range 0.15 to 0.8. The corresponding Reynolds numbers were 8,400 and 45,000. The results indicate no significant change of the jet growth rate or centerline velocity decay compared to the undisturbed free-jet. The mechanical forcing system consists of two counter-rotating hexagonal cylinders located parallel to the span of the nozzle. Forcing frequencies up to 1,500 Hz were tested. Both symmetric and antisymmetric forcing can be implemented. The results for antisymmetric forcing showed a significant (75 percent) increase of the jet growth rate at an exit Mach number of 0.25 and a Strouhal number of 0.019. At higher rotational speeds, the jet deflected laterally. A deflection angle of 39° with respect to the centerline was measured at the maximum rotational speed.

ACKNOWLEDGEMENTS

TABLE OF CONTENTS

page

LIST OF FIGURES

LIST OF TABLES

NOMENCLATURE

d	Jet exit width
f	Excitation frequency
M	Mach number
p	Pressure
Re	Reynolds number
St	$=f \cdot d/U_{ex}$, Strouhal number
St_l	$=f \cdot \delta/U_{\mathfrak{C}}$, local Strouhal number
U	Downstream velocity component
u'	Downstream velocity component rms value
V	Hot-wire voltage output
x	Downstream coordinate
y	Lateral coordinate
α	Jet deflection angle
δ	Velocity profile width
μ	Viscosity
ρ	Density
ω	Cylinders' rotational speed

Subscripts

$\dot{\mathfrak{C}}$	Centerline condition
ex	Nozzle exit condition
o	Nozzle stagnation condition
pp	Peak-to-peak value
rms	Root mean square
s	Static condition
t	Total condition

1. INTRODUCTION

It has been shown in a number of experimental investigations that the growth rate of a two-dimensional turbulent jet can be increased by the action of a superposed acoustical field or other forcing techniques.[1-5] This increased growth rate is of considerable interest in a number of practical problems where rapid mixing of mass, momentum or energy of the jet with its surroundings is important. Most investigations on forced two-dimensional jets have been limited to small amplitude excitation of low speed jets. These investigations focussed on the turbulent structure of the jet.[1-3] A few investigations have also been conducted with large excitation amplitudes. They are limited, however, to low frequencies due to limitations of the forcing systems used.[4,5]

A schematic diagram of the two-dimensional jet is shown in Figure 1. The non-dimensional parameters characterizing this flow are the Reynolds number Re $= (\rho U)_{ex} \cdot d/\mu$, the Strouhal number St $= f \cdot d/U_{ex}$ and the Mach number M_{ex}. In addition, the symmetry of the disturbance field plays an important role in the subsequent development of the jet.[2] Two different forcing modes are apparent: a symmetric forcing mode in which the traverse velocity component of the disturbance is symmetric with respect to the geometrical plane of symmetry of the flow, and an antisymmetric forcing mode where the disturbance is antisymmetric with respect to this plane. Available data indicates that symmetric forcing of a two-dimensional jet results in significant growth rate increases for a limited range of Strouhal numbers, $0.25 < St < 0.5$.[3] These results were obtained with small amplitude acoustical excitation. The behaviour of the jet under large amplitude symmetric excitation has not been documented. Axisym-

- 1 -
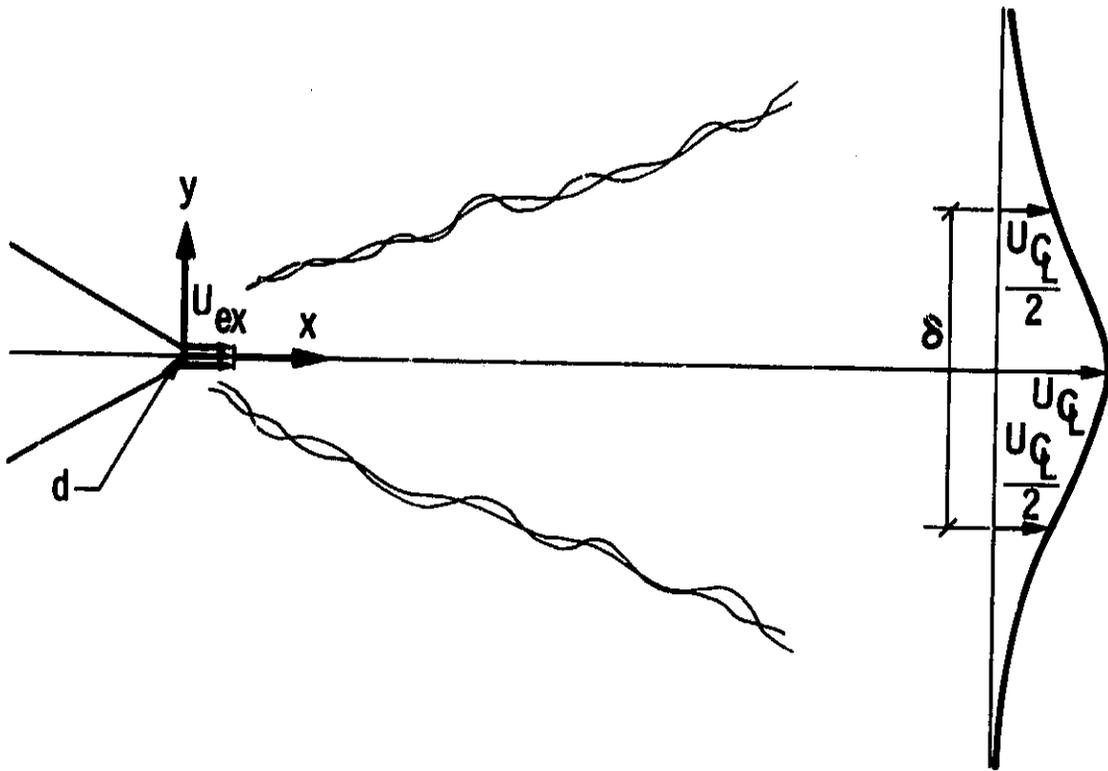
Figure 1. The two-dimensional jet.

metric jets do show significant growth rate increases under large amplitude mass flow oscillations at a wider Strouhal number range.[6] Furthermore, inviscid stability analyses predict growth of both symmetric and antisymmetric disturbances.[7] Antisymmetric forcing of two-dimensional jets results in large increases of the growth rate[2] at moderate Strouhal numbers (St<0.02). The large growth rates, however, do not necessarily imply increased small scale mixing.[2] At very low Strouhal numbers, the entire jet flaps with the local width of the free-jet.[4]

In the present investigation, we address the effect of forcing technique, frequency and amplitude of the excitation on the far-field development of a high speed jet. Pitot tube profiles were obtained at several downstream locations, jet exit Mach number and at various frequencies and amplitudes of the oscillations. In a second series of experiments, the effect of large amplitude antisymmetric forcing on the jet flow field was investigated. Because of the low excitation amplitude attainable by acoustical forcing, we opted for a mechanical system. Our design objective was to reach excitation frequencies of the order of 1,000 Hz and amplitudes comparable to those used in References 4 and 5. This was accomplished by using a pair of counter-rotating hexagonal cylinders located parallel to the nozzle edges. However, at the high rotational speeds necessary to achieve the design frequency, the interaction between the cylinders and the jet resulted in lateral deflection of the jet. This new phenomenon prevented us from conducting systematic parameter variations. Therefore, a preliminary evaluation of the flow field was conducted and measurements of the main features of the flow are reported.

2. FLOW FACILITY AND INSTRUMENTATION

The experiments reported here were conducted in the facility shown in Figure 2. A schematic diagram of the facility is presented in Figure 3. The facility uses pressurized shop air as working fluid. The high pressure air is first regulated down to the operating pressure by a remotely operated dome regulator. An orifice plate downstream of the regulator is used to monitor the mass flow through the system. An accumulator and a pneumatic oscillator are located downstream of the orifice plate; both are needed for the mass flow oscillation tests. The two-dimensional jet nozzle is located downstream of these components. Air enters the nozzle through two perforated tubes along the entire span of the nozzle. A perforated plate and honeycomb section are used to reduce the turbulence level and non-uniformity of the stream. They are followed by a 20 to 1 two-dimensional contraction. The nozzle exit has a cross-sectional area 2.54 mm by 169 mm, with the large dimension being along the span direction. The flow was confined in the spanwise direction by two end-plates. The plates were made of lucite for shadowgraph flow visualization. The end-plates extended 0.61 m downstream of the nozzle exit. The facility can be operated up to a maximum pressure ratio of 2.0, i.e., $M_{ex} \simeq 1.0$. A number of validation tests were conducted at exit Mach numbers of 0.3, 0.5, 0.7 and 0.9. The results are reported in the next section.

The mass flow oscillations were introduced with the help of an electro-pneumatic oscillator located upstream of the nozzle as shown in Figure 3. The oscillator is driven by a wave generator and a power amplifier. It modulates the mass flow through the system at the desired frequency and amplitude by

- 4 -
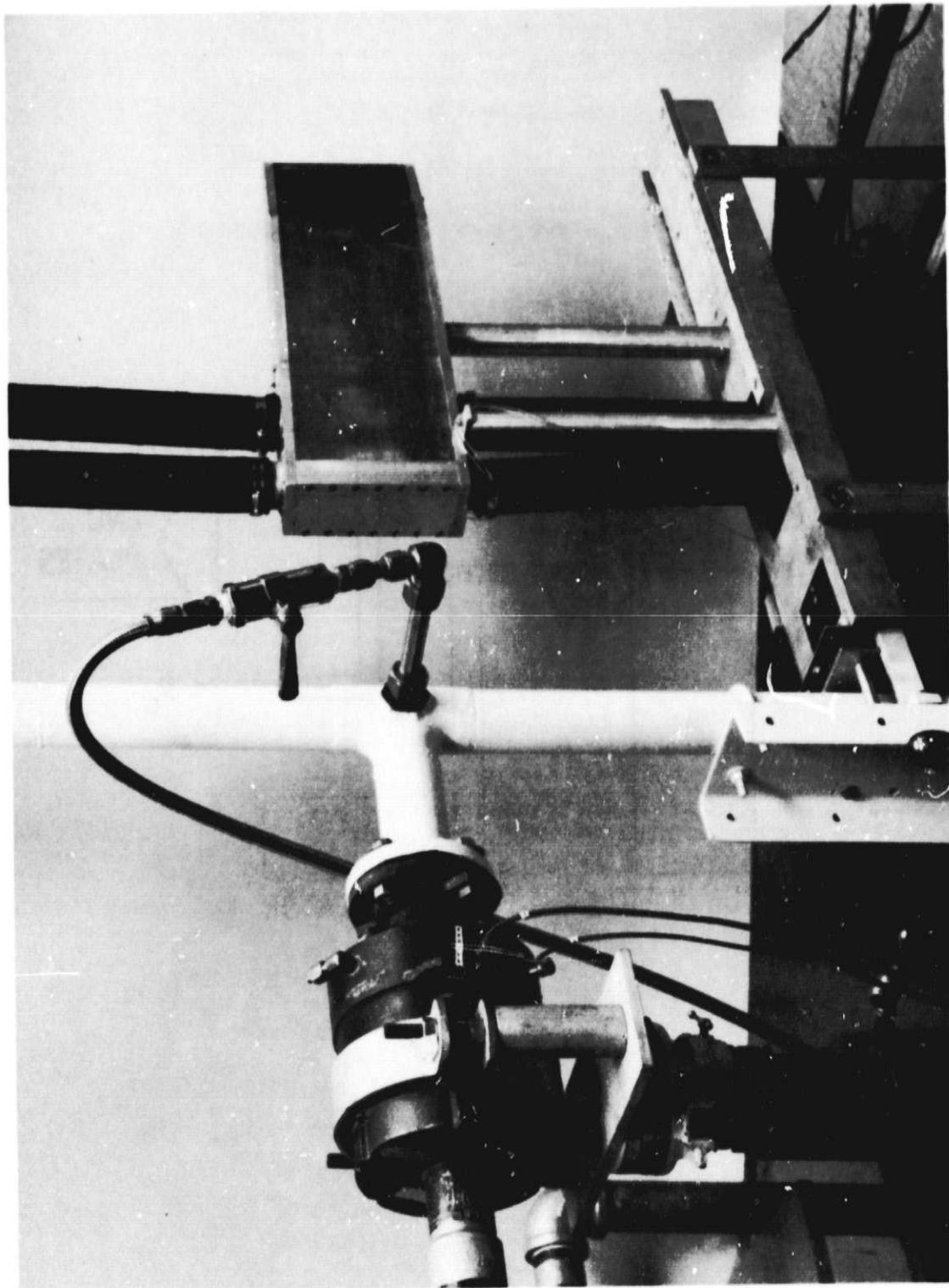
Figure 2. Two-dimensional jet facility.
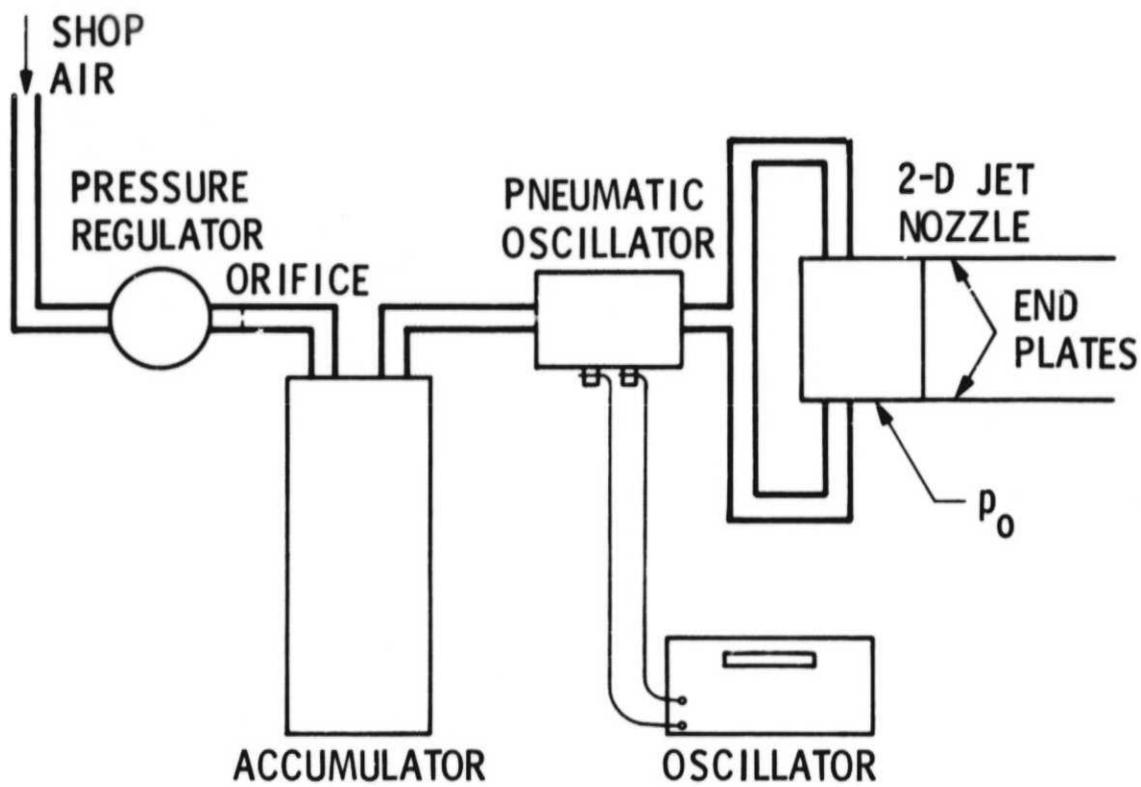
Figure 3. Schematic diagram of two-dimensional jet facility.

means of a variable area orifice. In the large amplitude mass flow oscillation tests, the mean mass flow was kept constant in order to provide a good reference for comparison. The accumulator was needed to isolate the measured pressures on the orifice from the pressure fluctuations induced by the mass flow oscillations.

Tests were conducted to characterize the operation of the system with mass flow oscillations. For a fixed exit velocity as the frequency was varied, several system resonances were observed. They were characterized by hot-film measurements of the velocity at the nozzle exit. The results, summarized in Table 1, were the maximum rms value of the fluctuation normalized with the local mean. The results presented are at the resonant frequencies and three

Table 1

Flow Facility Resonances

f(Hz)	$M_{ex}=0.3$ V_{rms}/V	$M_{ex}=0.5$ V_{rms}/V	$M_{ex}=0.68$ V_{rms}/V
56	0.032	0.01	---
270	0.036	0.011	---
356	0.031	0.011	---
397	0.018	---	---
480	0.013	0.0049	0.0058
572	0.01	0.0047	0.0065
642	0.009	0.0047	0.0058
768	---	---	0.0005
846	0.004	---	0.0004

exit Mach numbers. The maximum normalized amplitude at various resonant frequencies decreases as the frequency or Mach number is increased. Based on these results, the test conditions indicated in Table 2 were selected. Both the rms value of the velocity fluctuation, u', and the peak-to-peak amplitude normalized with the mean velocity are given in Table 2. Note that at the highest Mach number and at the highest frequency, only the low amplitude excitation could be tested.

Table 2
Summary of Tests
Mass Flow Oscillations

f(Hz)	$M_{ex}=0.15$		$M_{ex}=0.5$		$M_{ex}=0.8$	
	u'/U	Upp/U	u'/U	Upp/U	u'/U	Upp/U
0	0.002	---	0.002	---	0.018	---
56	0.030	0.09	0.031	0.09	0.023	~0.05
	0.150	0.43	0.060	0.17	---	---
325	0.030	0.09	0.032	0.09	0.020	~0.05
	0.175	0.49	0.053	0.15	---	---
900	0.032	0.09	0.008·	0.02	0.019	~0.05

A number of tests were also conducted with a mechanical forcing system. The design objectives of this system were to achieve excitation frequencies of the order of 1,000 Hz and as large an amplitude as possible. The system consists of two counter-rotating hexagonal cylinders located parallel to the nozzle edges as shown in Figure 4. As each vertex of the hexagon moves into the
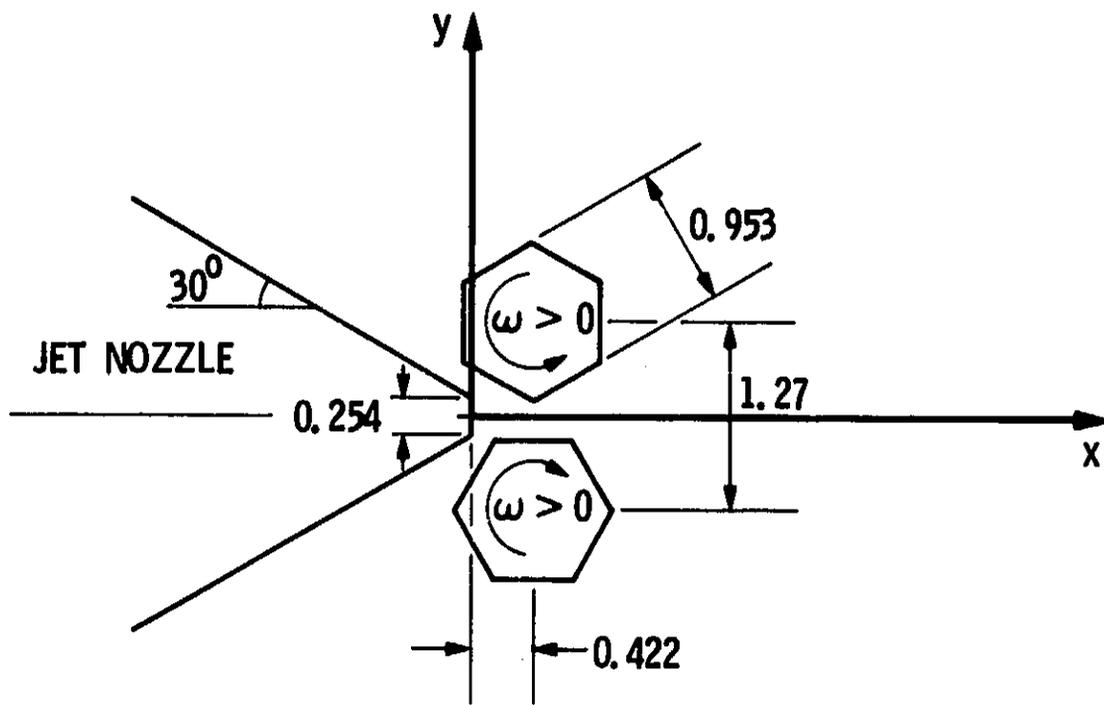
Figure 4. Mechanical forcing system schematic. Dimensions in cm.

jet, it introduces a disturbance. Thus, a rotation of the cylinders results in a periodic disturbance of the jet. Further, the six vertices per turn significantly reduce the rotational speed necessary to reach a given frequency. It was felt that the maximum amplitude of the disturbance would be obtained by arranging for the side of the hexagon to remain outside of the jet while the vertex moves into the jet shear layer. Based on this assumption, the geometrical parameters given in Figure 4 were chosen. This mechanical system was attached to the nozzle. A picture of the attachment is presented in Figure 5. Front and side view pictures of the facility with the attachment mounted are presented in Figures 6 and 7, respectively.

The cylinders were driven with a variable speed DC motor. A gear box was used to increase the rotational speed by a factor of six. The actual maximum rotational speed tested was 15,000 rpm which corresponds to an excitation frequency of 1,500 Hz. This speed is significantly lower than the first mechanical resonance of the system, estimated at 40,000 rpm. The cylinders could be rotated in both directions, always counter-rotating with respect to each other. The direction indicated in Figure 4 is the preferred (positive) direction because the cylinders and the fluid move in the same direction during the interaction, thus minimizing the load on the system. A few exploratory tests were conducted with the cylinders rotating in the negative direction. With this system, the relative phase between the two cylinders could also be varied. The phase shown in Figure 4 corresponds to antisymmetric forcing because the maximum disturbance in one shear layer corresponds to minimum disturbance in the other. Symmetric forcing can be obtained by rotating one cylinder 30° with respect to the other from the position depicted in Figure 4. Only a few tests were conducted in the symmetric configuration. The tests conducted in this system were primarily exploratory tests aimed at characterizing the
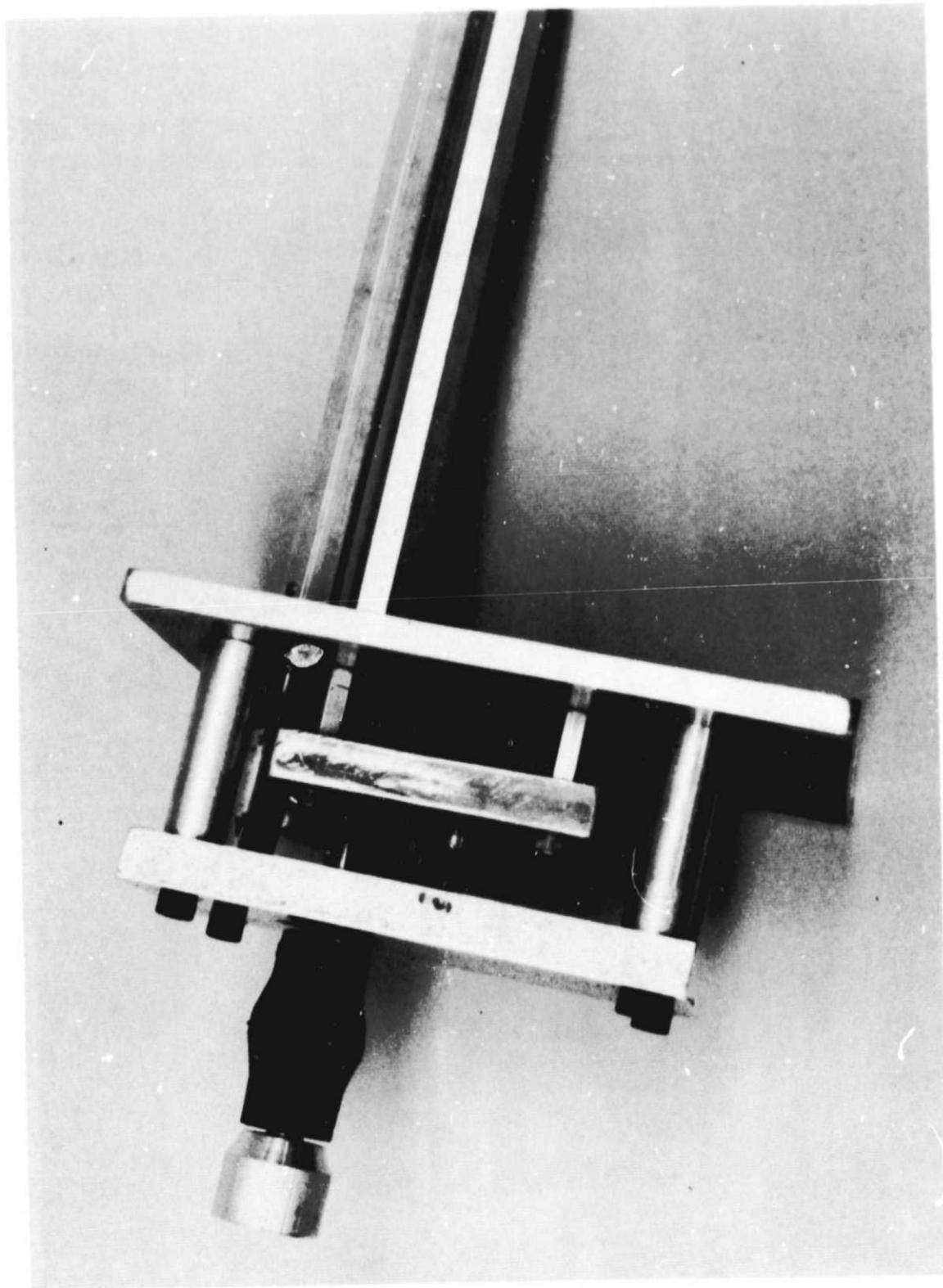
Figure 5. Mechanical forcing system hardware.
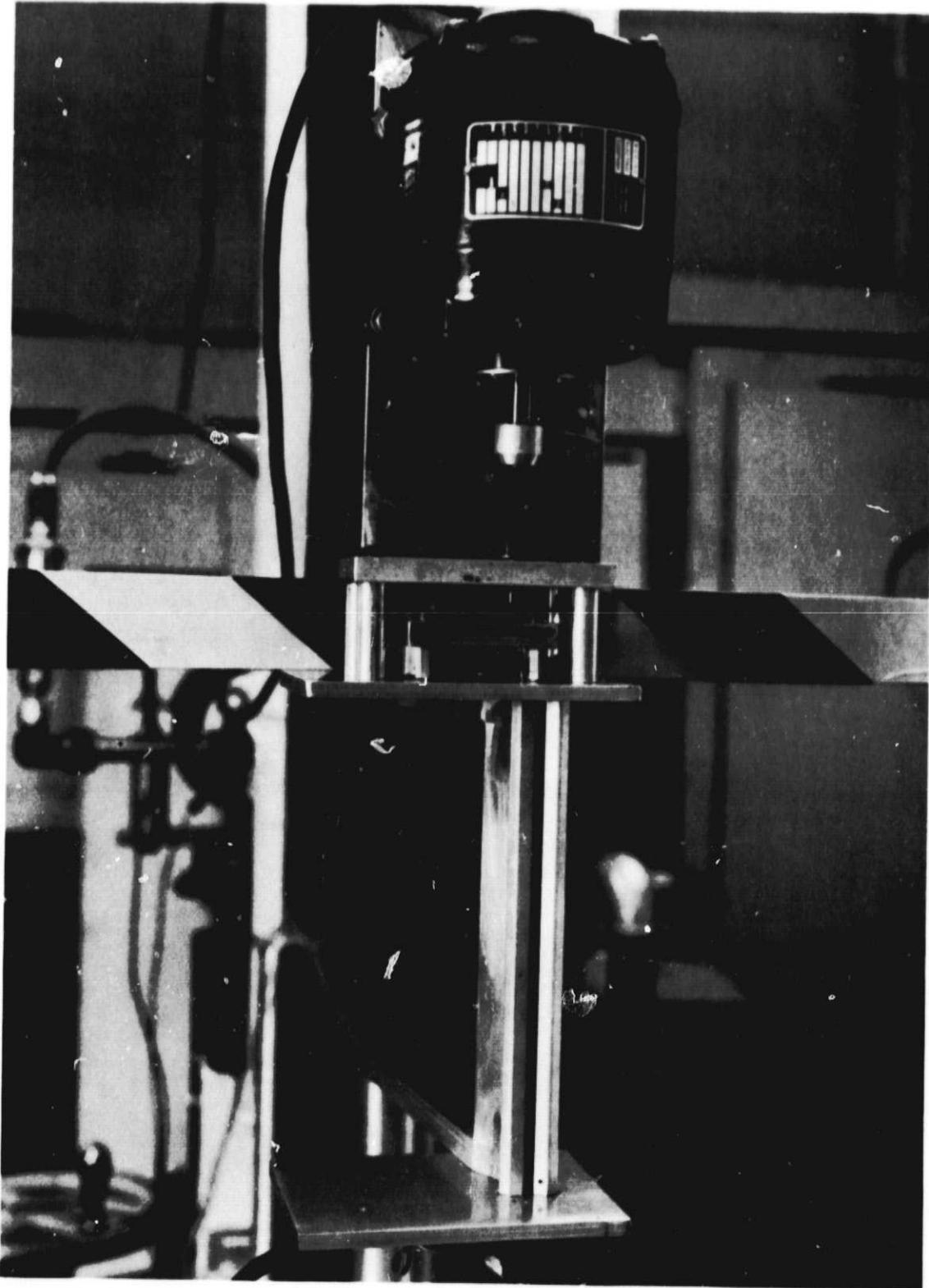
Figure 6. Front view, mechanical forcing system.
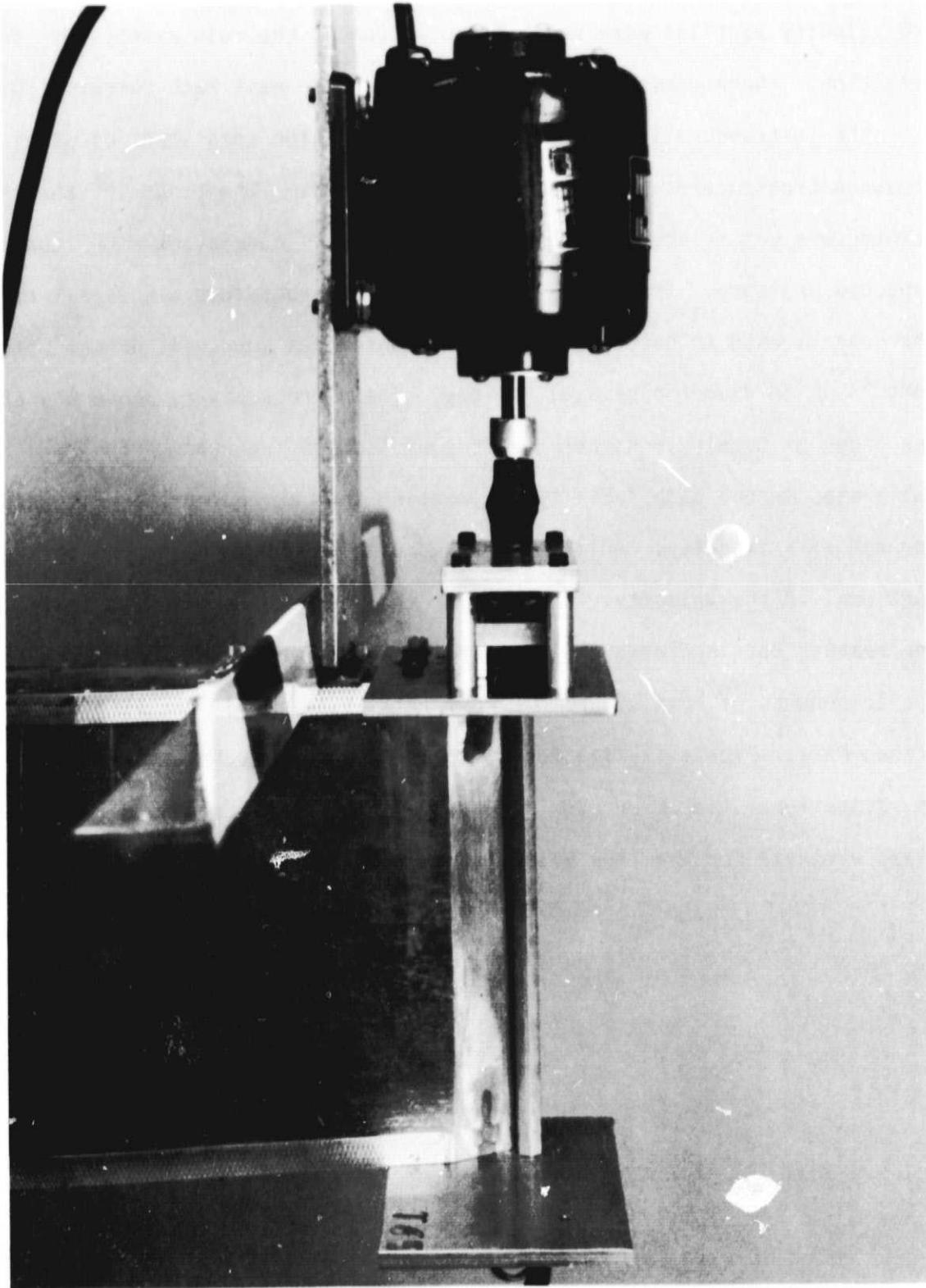
Figure 7. Side view, mechanical forcing system.

interaction between the rotating cylinders and the jet. Shadowgraph pictures and velocity profiles were obtained to document the main aspects of this interaction. These measurements were limited to an exit Mach number of 0.25.

The instrumentation used in this investigation consisted of strain-gauge pressure transducers and a hot wire anemometer. The range of the pressure transducers was selected for maximum sensitivity consistent with the maximum expected pressure. The Pitot tube profiles were obtained with a X-Y recorder. The sensors used in hot wire velocity measurements were cylindrical film sensors 25 μm in diameter by 0.51 mm long. Their frequency response was at least one order of magnitude higher than the excitation frequency. The sensors were calibrated in the same facility by locating them at the nozzle exit and varying the exit velocity. A linearizer was used to obtain an output voltage proportional to the velocity. Except for the results presented in Table 1, all the results obtained with the hot wire anemometer used the linearized output. The components of this system are commercially available and will not be described here. Flow visualization by the shadowgraph technique was used in this investigation. In order to increase contrast, pure carbon dioxide gas was mixed with air for the flow visualization tests.

3. RESULTS

3.1 Free-Jet

A number of tests were conducted on the undisturbed free-jet to obtain base data for comparison with forced jet results and with the results of other investigators as well.   These tests consisted of Pitot tube traverses on the mid-span plane at several downstream positions and exit Mach numbers. The jet exit Mach numbers tested and the corresponding Reynolds numbers are given in Table 3. From the Pitot tube profiles the centerline total pressure evolution was obtained.   These results are presented in Figure 8.   In this figure, the nozzle total pressure divided by the centerline total pressure is plotted as a function of downstream distance. It is apparent that the jet exit Mach number does not influence this parameter.   For a self-similar jet, a linear increase of this parameter with downstream distance is expected.   The results, presented in Figure 8, show this linear trend for x/d>10. A straight line fit to the data downstream of this position gives

$$(P_o - P_s)/(P_t C_L - P_s) = 0.216 \ (x/d-17.56)$$

The standard deviation from this line is 0.859 for all the data, at various Mach numbers.

Table 3

Free-Jet Test Conditions

| M_{ex}	0.3	0.5	0.7	0.9
$Re(x10^{-4})$	1.7	2.8	3.9	5.0

- 15 -
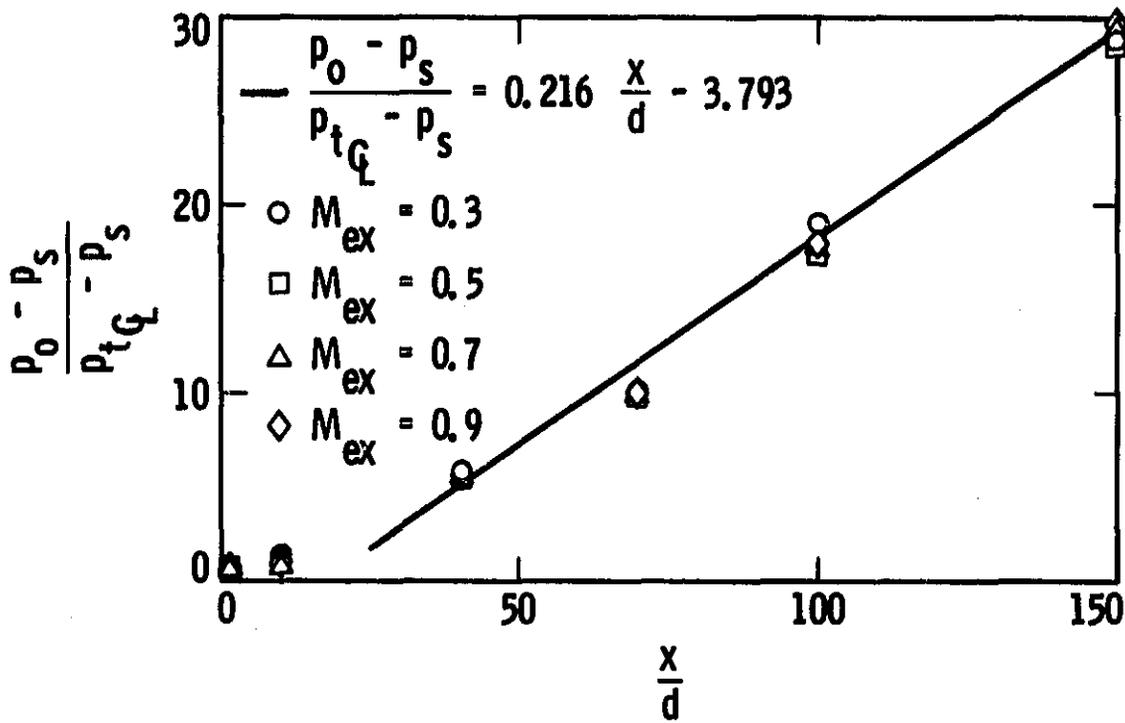
Figure 8. Centerline total pressure evolution for free-jet.

The results on the free-jet growth rate are presented in Figure 9. In this figure, the profile width, δ (see Figure 1 for its definition), normalized with the nozzle exit width, is plotted as a function of normalized downstream distance. Here again, self-similarity requires a linear dependence of δ on x. This behavior is found in the far field x/d>10. Mach number effects are within the scatter of the data. A straight line fit to the data gives

$$\delta/d = 0.179 \ (x/d) + 0.25$$

The standard deviation from this line is 0.445.

These results are in good agreement with the results of other investigations.[8-10] There is, however, considerable scatter among those results (see, for example, Reference 10 for a compilation of two-dimensional jet results). Only the velocity virtual origin, x/d=17.56, is somewhat higher than reported values. Yet values for this parameter, from 13 to -13, can be found in the literature.[10]

3.2 Mass Flow Oscillations

Systematic variation of various parameters was conducted to determine the effect of mass flow oscillations on the mean flow field. These tests included changes of the jet exit Mach number, oscillation frequency and amplitude. The conditions tested are given in Table 2. The Strouhal and Reynolds numbers corresponding to these conditions are given in Table 4. For each of these conditions, total pressure profiles were obtained at three downstream locations. Throughout these tests, the mean mass flow at each Mach number was maintained constant. At the lower Mach numbers, the pressure readings on the metering orifice were maintained within 2 percent. At $M_{ex}=0.8$, the imposed mass flow oscillations altered the operating point of the facility, resulting in a 10 percent scatter of the orifice pressure readings.
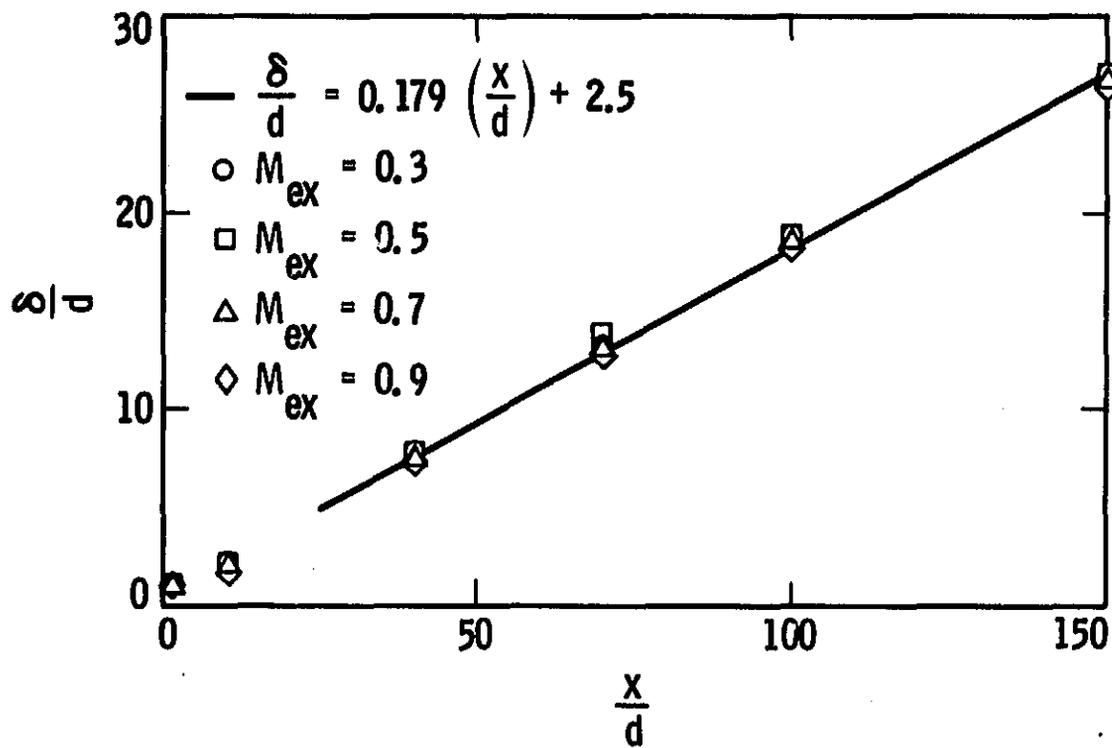
Figure 9.   Free-jet growth rate.

Table 4

Mass Flow Oscillation Tests

Non-dimensional Parameters

M_{ex}	0.15	0.5	0.8
$Re(\times10^{-4})$	0.84	2.8	4.5
f	St	St	St
56	0.0028	0.00084	0.00052
326	0.016	0.0048	0.0032
900	0.045	0.013	0.0084

The amplitude of the velocity fluctuations at the jet exit were varied from 10 percent to 50 percent of the mean (Table 2). At low amplitudes, the velocity variation, with time, approached a sinusoidal waveform. At high amplitudes, significant departures from the pure sinusoidal waveform were found. No attempt was made to characterize these departures. The velocity signal was free from high frequency noise at the lower Mach numbers. At the highest exit Mach number, however, the high frequency noise amplitude was comparable to the excitation amplitude.

The results of several pitot traverses at x=25 cm and exit Mach number 0.15 are presented in Figure 10. Two traverses obtained at the same conditions are superimposed on each graph. Comparison among the various curves in this figure shows no significant effect of mass flow oscillation frequency or amplitude on the pitot tube profiles. The results at different Mach numbers and downstream positions are presented in Figures 11 and 12 for the centerline total pressure and the profile width, respectively. In these figures the results obtained at different frequencies and amplitudes for each Mach number
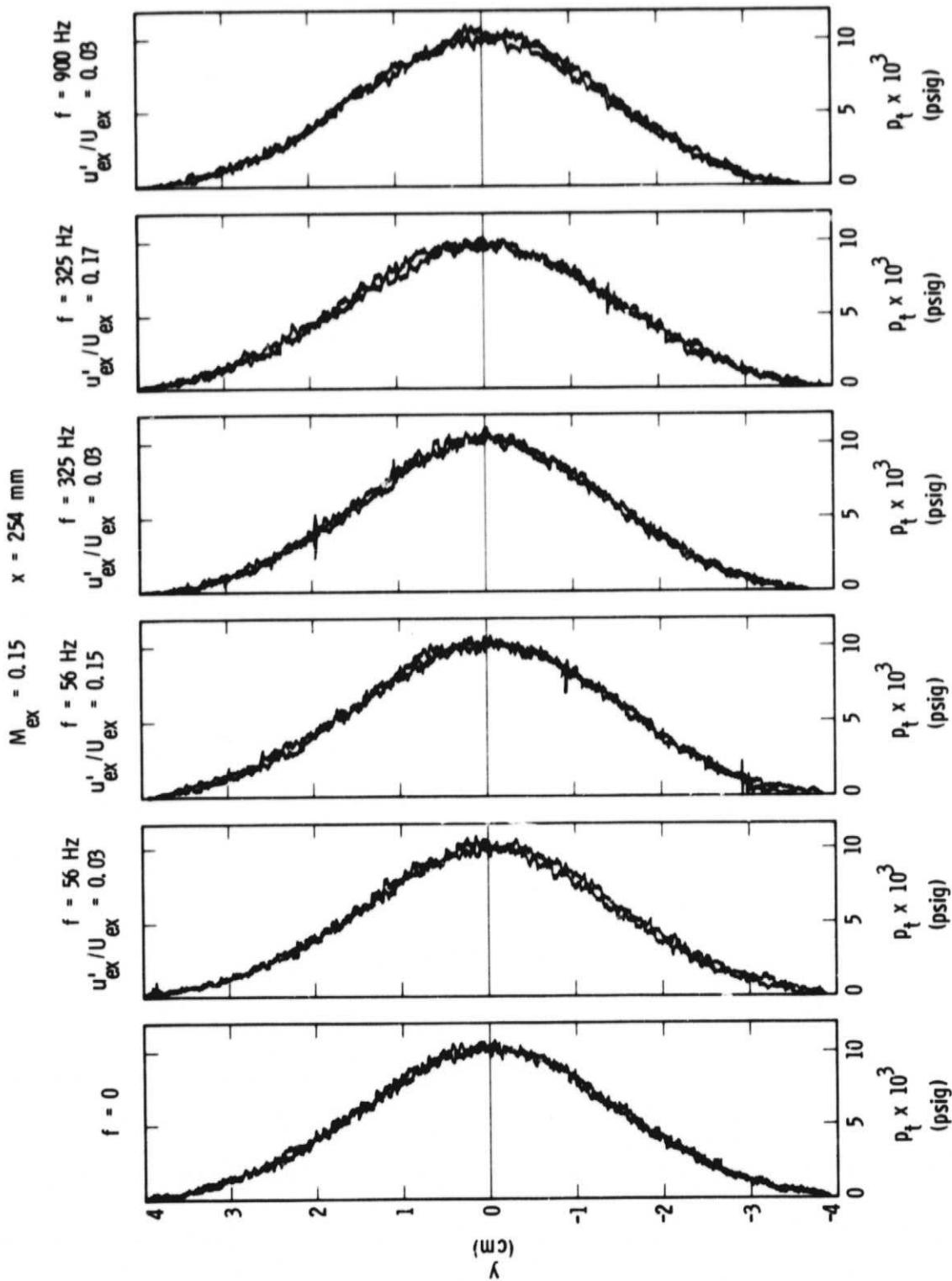
Figure 10. Total pressure profiles for mass flow oscillation. x = 254 mm.
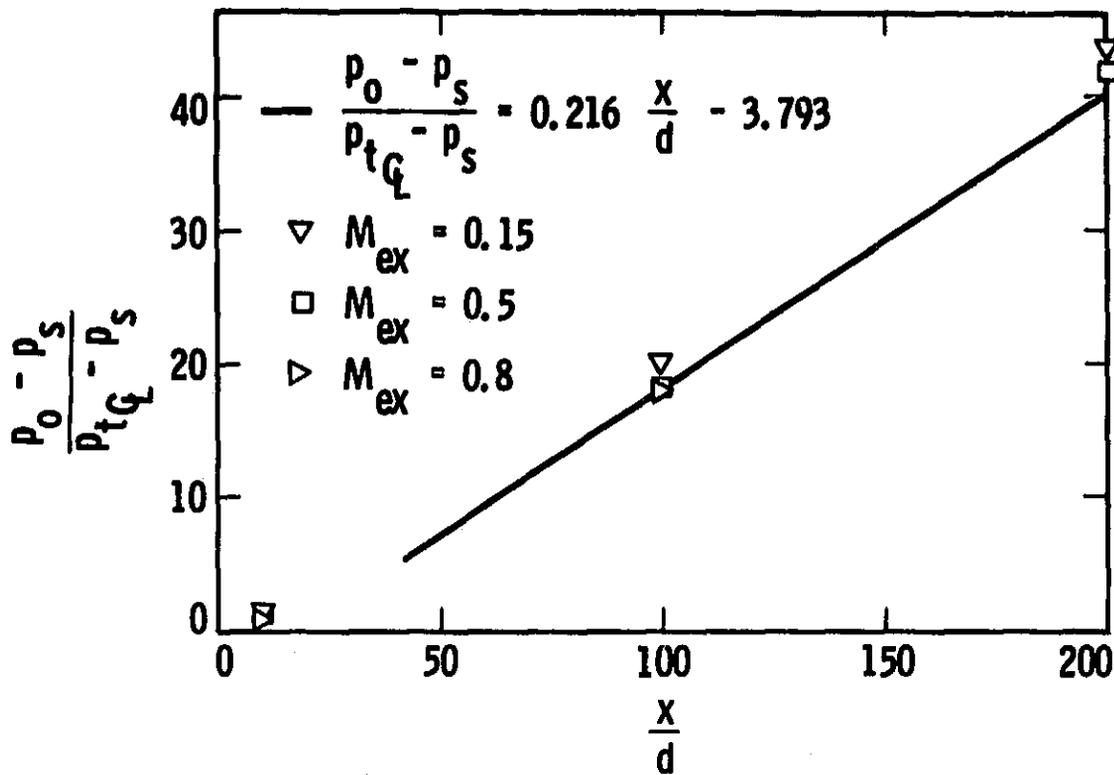
Figure 11. Centerline total pressure evolution for mass flow oscillations.
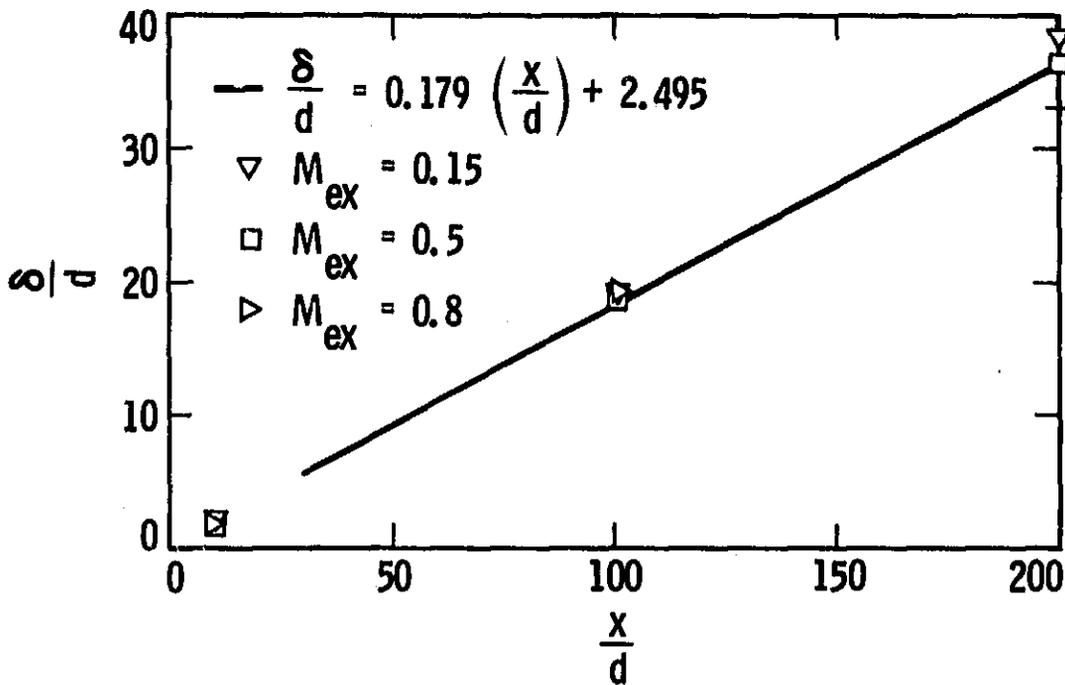
Figure 12. Jet growth rate for mass flow oscillations.

are shown as a single point. Also plotted in these figures are the fitted lines obtained from the free-jet data. It is apparent from these results that mass flow oscillations have no significant influence on the two-dimensional jet growth rate at Strouhal numbers St<0.05 even at excitation amplitudes 50 percent of the mean.

3.3 Mechanical Excitation

Because of the lack of sensitivity of the two-dimensional jet to symmetric excitation shown by the mass flow oscillation results, the main emphasis of this part of the research was on the antisymmetric forcing mode. A measure of the excitation amplitude of the antisymmetric mode is the deflection of the jet caused by the cylinders under static conditions. These results are presented in Figure 13. The two limiting cases are shown in this figure as Case A and Case B, respectively. Case A is characterized by the cylinders having sides parallel to each other forming an angle of -15° with the downstream direction, while in Case B the angle is 15°. The hot wire velocity profiles at x=25 cm for the free-jet, Case A and Case B are shown in this figure. It is apparent that the significant effect of the cylinders is a lateral deflection of the jet in the negative or positive y-direction for Case A or B, respectively. The width of the jet or centerline velocity are not significantly modified by the presence of the cylinders. The effective deflection angle, α, can be defined from these profiles as

$$\alpha = \arctan\ (y_{max}/x)$$

where y_{max} is the location of the maximum velocity. Using this definition we find $\alpha = -12''$ and $\alpha = 16°$ for Case A and B, respectively. These values can be compared to the values of $\pm 30°$ used in Reference 4.

- 22 -
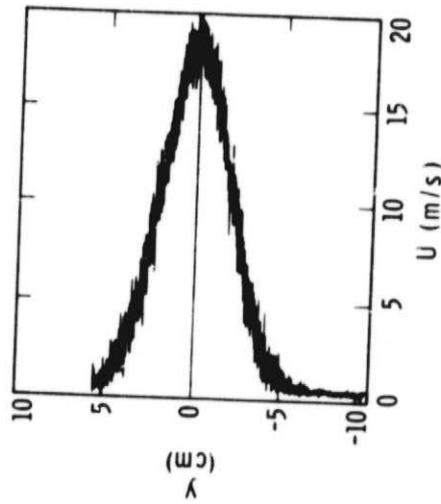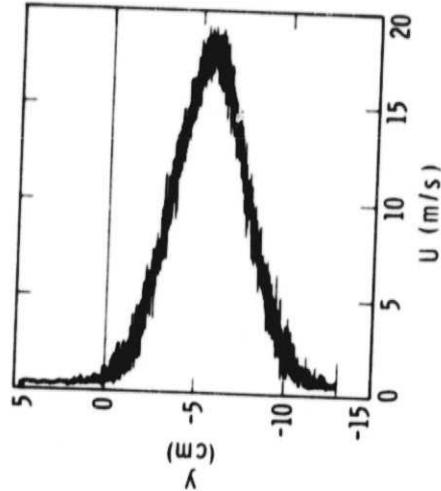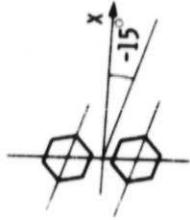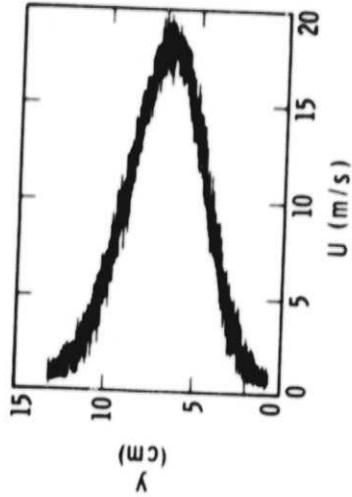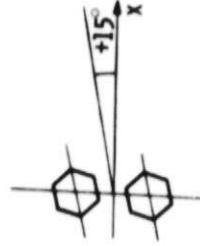
Figure 13. Static effects for mechanical forcing system.

The effect of positive rotational speed ($\omega > 0$) at x=25 cm is presented in Figure 14. At low speeds of the cylinders, say 5,000 rpm, the velocity profile is typical of a forced jet, that is, the maximum velocity in the profile is considerably lower than the value for a free-jet while the width of the profile is increased significantly. At higher rotational speeds, 10,000 rpm or 15,000 rpm, the flow field changed entirely with the maximum velocity now located at y = -17 cm and -20 cm, respectively. These values correspond to lateral deflection angles α = -34° and -39°, respectively. The apparent preference for negative displacements was somewhat troublesome. However, the velocity profiles at 10,000 rpm and 15,000 rpm show increased velocity fluctuations at y = 7 cm and 17 cm compared to the centerline, respectively. Flow visualization revealed the flow configuration depicted in Figure 15. The jet splits on the mid-span plane with the upper half deflecting toward the positive y-direction and the lower half toward the negative y-direction. It was also found that small movement of the cylinders relative to the nozzle will alter the direction of the jets. It was, in fact, demonstrated that the entire jet could be deflected in either direction by small changes of the cylinders' position, of the order of a few tenths of a millimeter.

The rotational speed for the onset of jet deflection was dependent on the jet exit velocity. As the jet exit velocity was increased, the rotational speed for onset was also increased. Jet deflection was not observed with the cylinders rotating in the negative direction, that is, when the cylinders' direction is opposite to the jet flow direction at the point of contact.

The jet deflection phenomenon distracted us somewhat from the main objective of this investigation. The velocity profile at 5,000 rpm (500 Hz) in Figure 14 shows a significant increase in jet growth rate. Exploratory tests with $\omega < 0$ confirmed this result. However, when a symmetric configuration was
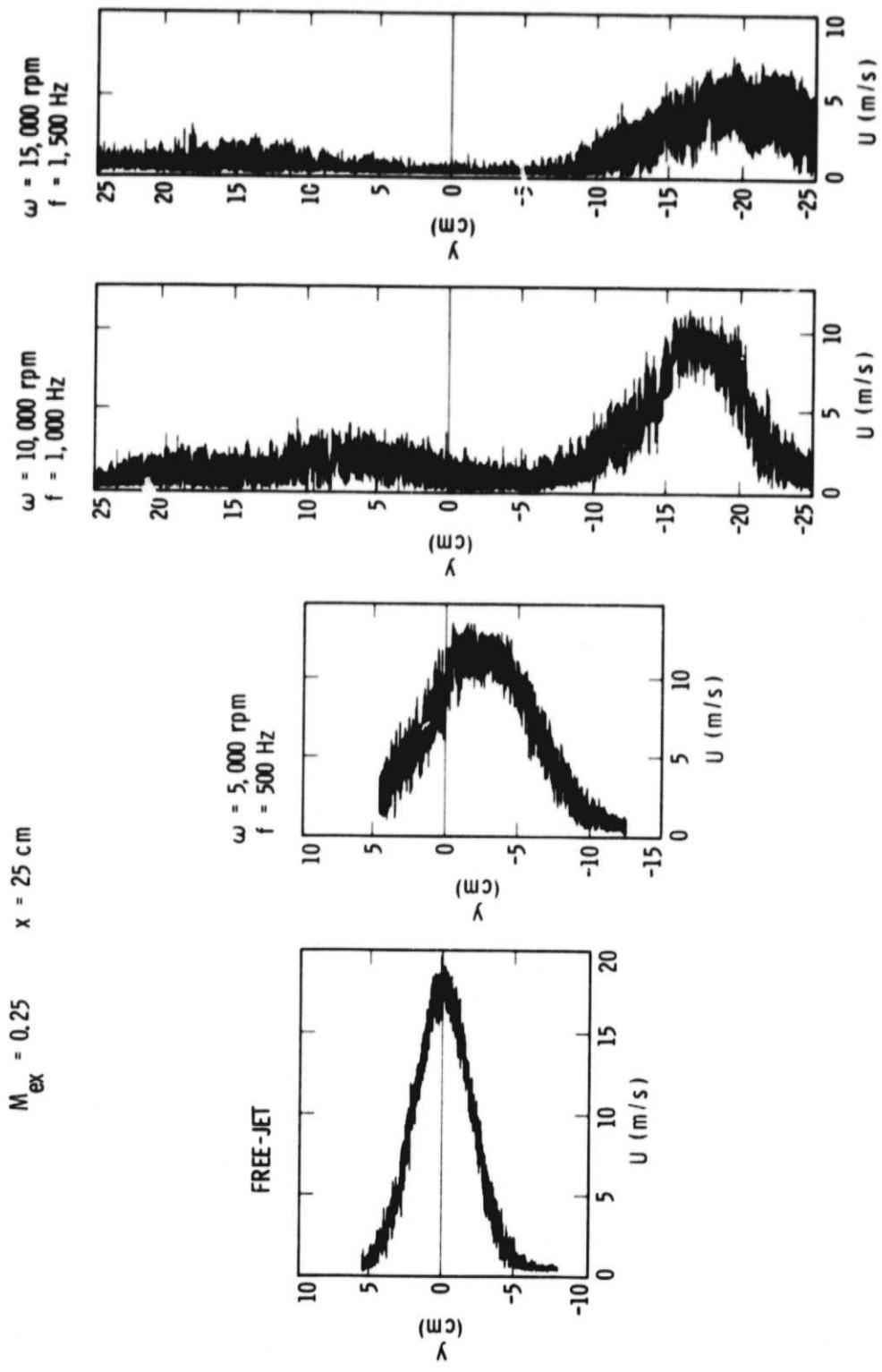
Figure 14. Effect of cylinders' rotational speed on jet development.
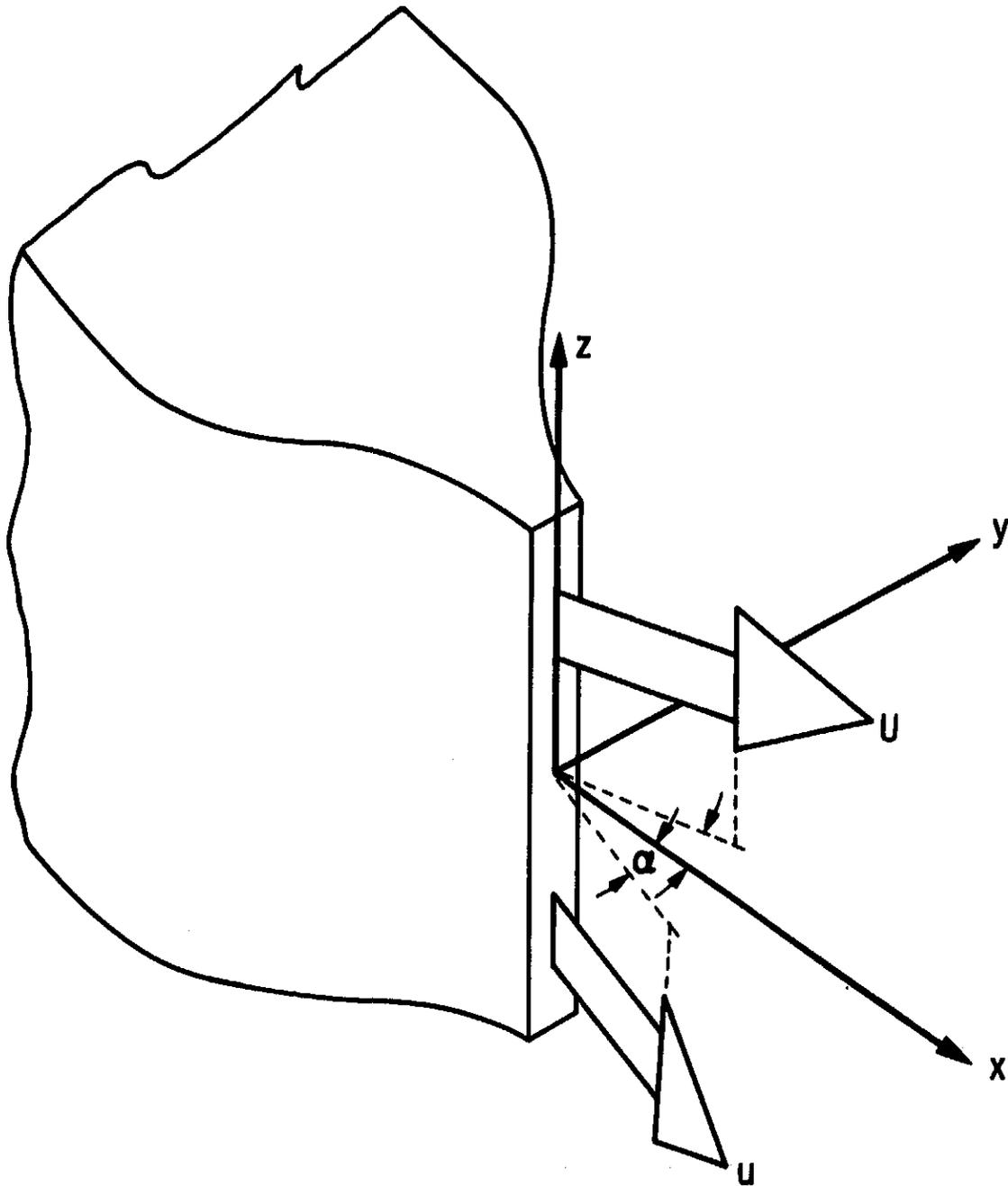
Figure 15. Flow field characteristics at high rotational speeds.

tested, no significant growth rate increase was found. No quantitative data were obtained in these cases. Shadowgraph flow visualization pictures of the free-jet, Figure 16, and of the excited jet, Figure 17, at M_{ex} = 0.25, St = 0.019 (500 Hz), show the growth rate increase in the latter. Furthermore, there is no evidence in this picture of a wavy jet structure found at lower Strouhal numbers.[4]

Comparison of these results with free-jet data is presented in Figures 18 and 19 for the centerline velocity decay and velocity profile width, respectively. For this comparison it has been assumed

$$(P_0 - P_s)/(P_{t\mathcal{L}} - P_s) = (U_{ex}/U\mathcal{L})^2$$

Also plotted in these figures are the results for the free-jet measured with the same equipment as the excited jet as well as the straight line fit found in the free-jet tests, Figures 8 and 9. The centerline velocity decay is reduced by 35 percent as compared to the free-jet. The profile width is increased by 75 percent.

Figure 16. Shadowgraph flow picture of the free-jet. $M_{ex} = 0.25$.
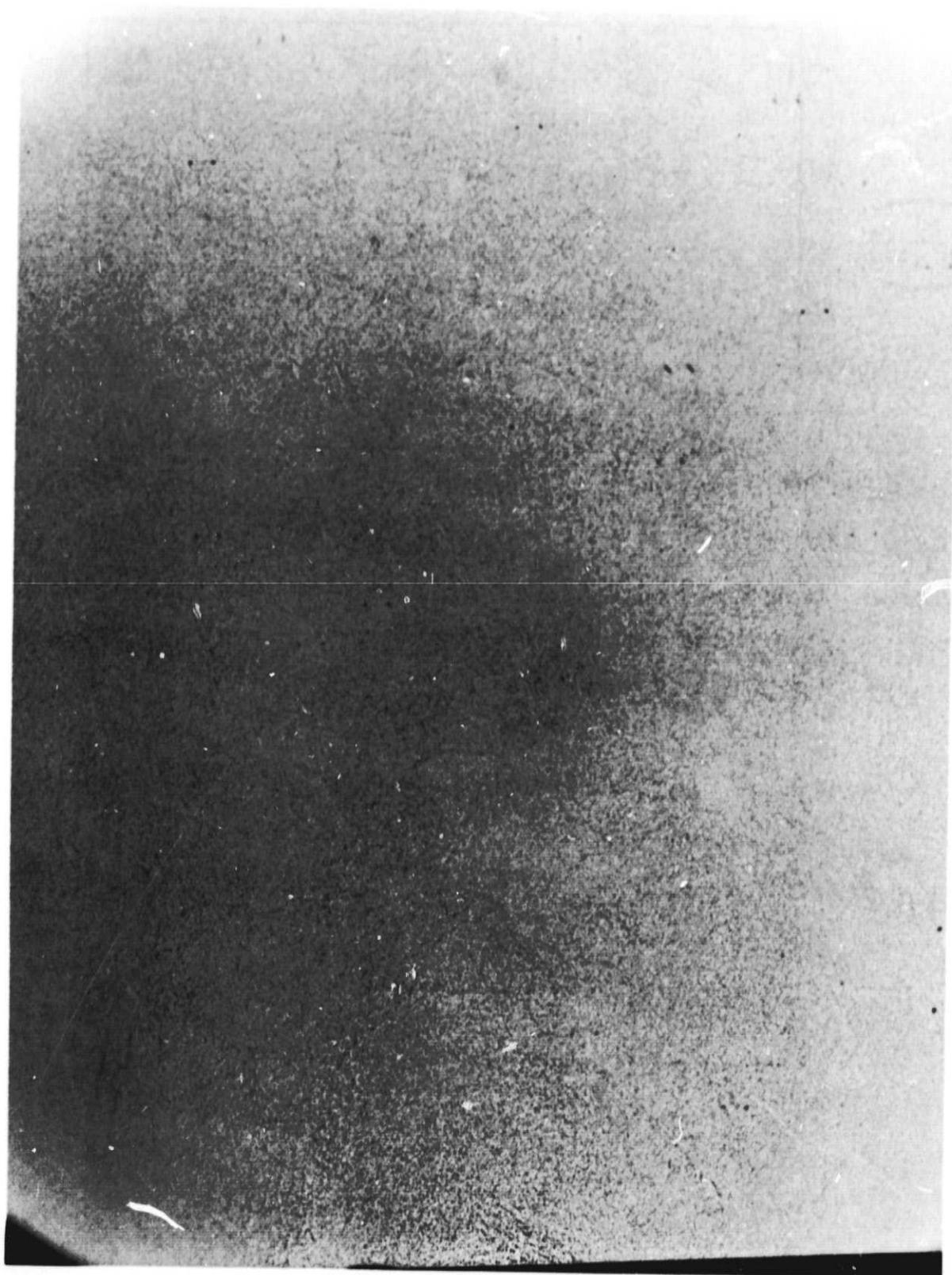
Figure 17. Shadowgraph flow picture of the forced jet. $M_{ex} = 0.25$, $St = 0.019$.
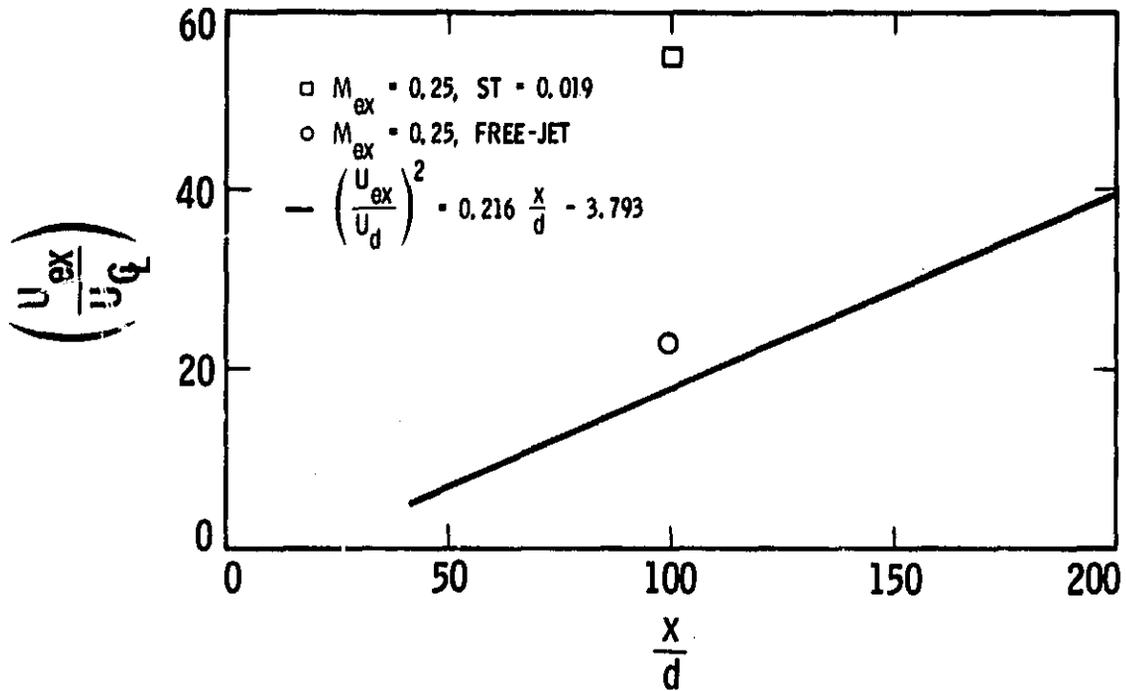
Figure 18. Centerline velocity evolution for mechanical forcing system.

$$\left(\frac{U_{ex}}{U_d}\right)^2 = 0.216\,\frac{X}{d} - 3.793$$

Legend:
- $\square$ $M_{ex} = 0.25$, $ST = 0.019$
- $\circ$ $M_{ex} = 0.25$, FREE-JET
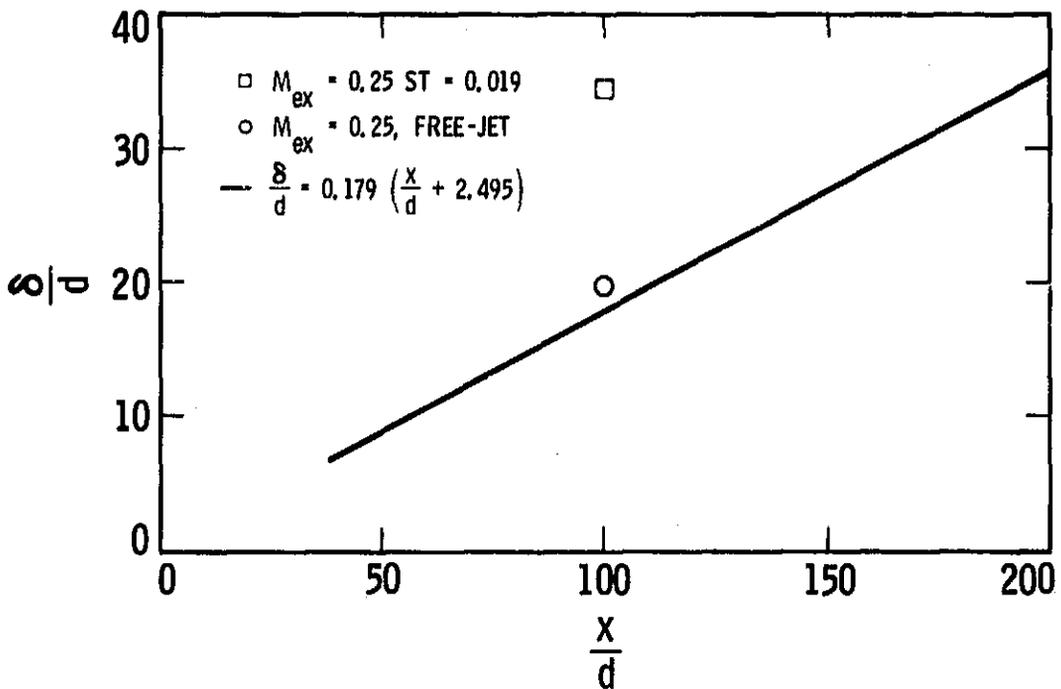
Figure 19. Jet growth rate for mechanical forcing system.

$$\frac{\delta}{d} = 0.179\left(\frac{X}{d} + 2.495\right)$$

Legend:
- $\square$ $M_{ex} = 0.25$ $ST = 0.019$
- $\circ$ $M_{ex} = 0.25$, FREE-JET

4. DISCUSSION

The effect of large amplitude forcing of a two-dimensional jet is seen to depend strongly on the symmetry characteristics of the excitation. Large amplitude mass flow oscillations do not alter the mean flow evolution in the Strouhal number range from 0.00052 to 0.045. On the other hand, antisymmetric forcing does result in a large increase of the jet width at comparable Strouhal numbers. This Strouhal number is based on jet exit conditions. A better indication of the dynamics of the flow can be obtained from the local Strouhal number, $St_1 = f \bullet \delta / U_{\mathbb{C}}$. This parameter is related to the jet exit Strouhal number by the expression

$$St_1 = C \bullet St \bullet (x/d)^{3/2}$$

where $C = 0.083$ from our free-jet data. In this equation we have neglected the location of the virtual origin; thus the equation is valid for $x/d \gg 1$. Strong interaction between the excitation and the jet turbulence can be expected to occur at values of the local Strouhal number of order one. The range of local Strouhal numbers covered in these tests is from $St_1 \ll 1$ to $St_1 \sim 1$ at values of $x/d \sim 100$. Therefore, the conditions for strong interaction were established for symmetric and antisymmetric disturbances. Our measurements indicate that only antisymmetric disturbances result in such a strong interaction. The selective amplification of antisymmetric disturbances by the two-dimensional jet is an indication of a large scale structure constituted by an axisymmetric vortex street. This possibility was first proposed in Reference 11. A characteristic local Strouhal number of 0.22 was reported for the large scale structure in that investigation. For the results presented in Figure

14, f = 500 Hz, St_1 = 1.5 at x/d = 100 and, using the above equation, St_1 = 0.22 at x/d = 27 are consistent with the observations reported in Reference 11.

It is interesting to compare our results with the predictions of stability theory. Results from stability theory have been used to describe the dynamics of the large scale structure in turbulent mixing layers.[12] However, for the two-dimensional jet, inviscid stability analysis predicts growth of both symmetric and antisymmetric disturbances at local Strouhal numbers below 0.3.[7] Maximum values of the amplification rate are found at local Strouhal numbers from 0.13 and 0.2, depending on the velocity profile chosen. Yet the present measurements indicate damping of symmetric disturbances. The results for antisymmetric forcing are consistent with inviscid stability theory. This conflict between inviscid stability theory and our results raises some questions as to the general applicability of the former to excitation of turbulent shear flows.

Using the counter-rotating cylinders in this investigation proved to be a valuable technique for two-dimensional jet forcing. The measured growth rate increases are larger than those found using acoustical forcing.[2] They are comparable to the ones obtained with the "flip-flop" nozzle[5] with the additional advantage in this case of improved small scale mixing at large Strouhal numbers. The possibility of self-induced excitation caused by releasing the cylinders from the driving mechanism was also demonstrated. The cylinders rotated freely under the action of the jet. The rotational speed was of the order of 1,000 rpm (100 Hz). The speed increased with the jet exit velocity. This self-excited condition is analogous to the operation of the "flip-flop" nozzle. In this case, however, the rotational speed is determined by balance

between aerodynamic friction on the surface of the cylinder and mechanical friction.

The jet deflection phenomenon observed at high rotational speeds is undoubtedly accompanied by rotation of the axis nozzle thrust. Although the thrust of the system was not measured, the thrust rotation angle should be comparable to the angles measured in the velocity field. The jet splitting phenomenon described in relation with Figure 15 is the result of the simultaneous interaction of both cylinders with the jet. If a single cylinder is considered, it can be expected that all the geometrical parameters as well as the jet exit velocity and its rotational speed will influence the jet deflection angle. Among these, the significance of the hexagonal shape of the cylinders needs to be determined. For a fixed geometry the relevant non-dimensional parameter is the ratio U_T/U_{ex}, where U_T is cylinder surface velocity. This parameter had a maximum value of 0.61 in these tests. At onset of the deflection its value was $U_T/U_{ex} = 0.2$.

5. CONCLUSIONS

Several conclusions were clearly established by the present investigation. Yet more tests of the mechanical system used in this investigation are required to fully evaluate its characteristics and potential applications. The main conclusions of this investigation are:

1. Symmetric forcing of a two-dimensional jet does not result in an increased growth rate at Strouhal numbers $0.00052 < St < 0.045$ and amplitudes up to 50 percent of the mean velocity.

2. Antisymmetric forcing does result in 75 percent increase of jet width. At the non-dimensional frequency tested in this investigation, $St = 0.019$, the growth rate increase is accompanied by increased mixing.

3. The use of two counter-rotating cylinders located at the jet exit is a unique technique to interact with the jet turbulence. Not only a significant increase in jet growth can be realized, but also significant jet deflection can be obtained.

6. REFERENCES

1. Brown, G.B. (1935) "On Vortex Motion in Gaseous Jets and the Origin of Their Sensitivity to Sound." Proceedings of the Physical Society, London, Vol. 47, no. 4, pp 703-732.

2. Fiedler, H., and Korschelt, D. (1979) "The Two-Dimensional Jet with Periodic Initial Conditions." Proc. 2nd Symposium on Turbulent Shear Flows, London.

3. Thomas, F.O., and Goldschmidt, V.W. (1983) "Interaction of an Acoustical Disturbance and a Two-Dimensional Jet: Experimental Data." J. Fluids Engineering, Vol. 105, pp 134-139.

4. Simmons, J.M., Platzer, M.F., and Smith, T.C. (1978) "Velocity Measurements in an Oscillating Plane Jet Issuing into a Moving Air Stream." J. Fluid Mech., Vol. 84, pp 33-53.

5. Viets, H. (1975) "Flip-Flop Jet Nozzle." AIAA J., Vol. 13, pp 1375-1379.

6. Sarohia, V., Bernal, L., and Bui, T. (1981) "Entrainment and Mixing in Pulsatile Ejector Flows." JPL Publication 81-36, Jet Propulsion Laboratory, Pasadena, California.

7. Sato, H. (1960) "The Stability and Transition of a Two-Dimensional Jet." J. Fluid Mech., Vol. 7, pp 53-80.

8. Bradbury, L.J.S. (1965) "The Structure of a Self-Preserving Turbulent Plane Jet." J. Fluid Mech., Vol. 23, pp 34-64.

9. Gutmark, E., and Wygnanski, I. (1976) "The Planar Turbulent Jet." J. Fluid Mech., Vol. 73, pp 465-495.

10. Chambers, F.W., and Goldschmidt, V.W. (1982) "Acoustic Interaction with a Turbulent Plane Jet." AIAA J., Vol. 20, pp 797-804.

11. Cervantes de Gotari, J., and Goldschmidt, V.W. (1980) "The Apparent Flapping Motion of a Turbulent Plane Jet--Further Experimental Results." ASME 80-WK/FE13, American Society of Mechanical Engineers, New York.

12. Ho, C.M. (1981) "Local and Global Dynamics of Free Shear Layers." In Numerical and Physical Aspects of Aerodynamic Flows, Ed. T. Cebeci, pp 521-533, Springer-Verlag, New York.